Common-mode Voltage Elimination of Three-level T-type Inverters With A Finite Control Set Model Predictive Control Method

Xiaodong Wang[1,2], Jianxiao Zou [1], Jiancheng Zhao[1], Zhenhua Dong[1], Min Wei[1], Xie Chuan[1], Kai Li[1]
(1. School of Automation Engineering, UESTC, Chengdu, 611731, China
2. Institute of Materials, China Academy of Engineering Physics, Mianyang, 621900, China
xiaodong0714@foxmail.com)

***Abstract*—The main contribution of this paper is the proposal of a new finite control set model predictive control (FCS-MPC) based method for three-level T-type inverters (3LT^{2}Is) to eliminate the common-mode voltage (CMV) with considering the dead time effects. Firstly, the CMV of the 3LT^{2}Is is analyzed and only six medium and one zero voltage vectors (6MV1Z) which generate zero CMV are defined as the candidate voltage vectors (VVs) for the FCS-MPC. Furthermore, the dead time effects when utilizing the defined candidate VVs with 6MV1Z are investigated and a new FCS-MPC based CMV elimination (CMV-EL) method is proposed. In the proposed CMV-EL method, the candidate voltage VVs are redefined by pre-excluding the VVs which will cause CMV fluctuations during the dead time from 6MV1Z. Besides, the proposed CMV-EL method can effectively eliminate the CMV as well as control the grid current and balance the neutral point potentials (NPPs). Finally, experimental results confirm the effectiveness of the proposed CMV-EL method.**

***Keywords*—Common-mode voltage(CMV), three-level T-type inverters(3LT^{2}Is), finite control set model predictive control(FCS-MPC), neutral point potentials(NPPs)**

I. INTRODUCTION

In recent years, the increasing demand for energy has stimulated the development of renewable energy generation, especially the photovoltaic power generation and wind power generation [1], [2]. Three-phase inverter is an important equipment for renewable energy sources connecting to the utility grid. Among various kinds of inverters, three-level T-type inverters (3LT^{2}Is) are most widely used, since 3LT^{2}Is basically combine the advantages of the two-level inverters such as low conduction losses and a simple operation principle with the positive aspects of three-level inverters such as low switching losses and superior output voltage quality [3], etc.

Traditional proportional-integral (PI) control with a pulse width modulation (PWM) block is most commonly used for inverters to provide controllable output currents [4]-[7]. However, large common-mode voltages (CMVs) are generated by fast switching operation and the dead time effects [8]-[10]. The existence of large CMVs lead to serious problems such as overvoltage stress to the winding of a motor and leakage currents in photovoltaic systems [11], [12]. Therefore, various CMV reduction strategies based PWM methods have been proposed in literatures [13]-[16]. However, these strategies inevitably complicate the PWM algorithm.

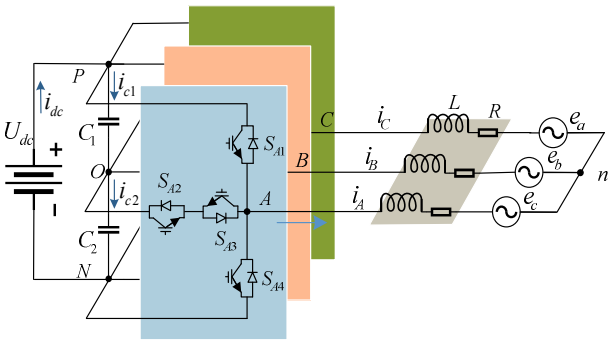

Fig. 1. Structure of the studied 3LT^{2}I

Finite control set model predictive control (FCS-MPC) has been demonstrated to be an optimization control scheme which is especially suitable for inverters since it has the advantages of simplicity and intuition, fast dynamic response, flexibility of control system constraints [10], [17]-[18]. FCS-MPC based CMV reduction strategies have been extensively studied for two-level inverters in [19]-[21]. It becomes more complicated for three-level inverters since there are more VVs. In [22], a model predictive control based method is proposed for 3LT^{2}Is to reduce the CMV and balance the NPPs for 3LT^{2}Is. However, dead time effects are not taken into account.

In light of this point, this paper proposes a new FCS-MPC based CMV elimination (CMV-EL) method for 3LT^{2}Is with considering dead time effects. The candidate VVs for the proposed CMV-EL method are redesigned by pre-excluding the VVs which will cause CMV fluctuations during the dead time zone. The proposed method can effectively eliminate the CMV as well as control the grid current and balance the neutral point potentials (NPPs). Experimental results are presented to verify the effectiveness of the proposed scheme.

This work was supported in part by the National Natural Science Foundation of China(No.51707030) and in part by Fundamental Research Funds for the Central Universities (No. ZYGX2015J075).

II. CONVENTIONAL FCS-MPC SCHEME FOR 3LT²IS

A. Average model of the 3LT²I

In order to simplify explanation, we assume that the bus voltage and the inductor currents are constant in a sampling interval and ignore the influence of dead time. The average model of the 3LT²I in two-phase stationary coordinate can be expressed as

$$\begin{bmatrix} i_\alpha(k+1) \\ i_\beta(k+1) \end{bmatrix} = A \begin{bmatrix} i_\alpha(k) \\ i_\beta(k) \end{bmatrix} + B \begin{bmatrix} u_\alpha(k) - e_\alpha(k) \\ u_\beta(k) - e_\beta(k) \end{bmatrix} \tag{1}$$

where i_α(k), i_β(k), u_α(k), u_β(k), e_α(k) and e_β(k) are the grid current, output voltage and grid voltage components of the 3LT²I in two-phase stationary coordinate at instant k, i_α(k+1) and i_β(k+1) are the predicted grid current at instant k+1, and A, B are shown as

$$\begin{aligned} A &= \begin{bmatrix} 1 - RT_s/L & 0 \\ 0 & 1 - RT_s/L \end{bmatrix} \\ B &= \begin{bmatrix} T_s/L & 0 \\ 0 & T_s/L \end{bmatrix} \end{aligned} \tag{2}$$

where T_s is the control period.

The dynamics of the DC link capacitor voltage is described by the differential equation shown as

$$\frac{dV_{cj}}{dt} = \frac{1}{C} i_{cj} \tag{3}$$

where V_{cj} (j=1,2) is the voltage of the DC link capacitor and C denotes the capacitor value. The capacitor voltage derivative dV_{cj}/dt is replaced by forward Euler approximation expressed as

$$\frac{dV_{cj}}{dt} = \frac{V_{cj}(k+1) - V_{cj}(k)}{T_s} \tag{4}$$

giving the discrete form of the DC link capacitor voltage shown as

$$V_{cj}(k+1) = V_{cj}(k) + \frac{1}{C} i_{cj}(k) T_s \tag{5}$$

where current i_{cj} (k) depends on the switching states and the grid currents of the 3LT²I, and can be calculated using the following expression:

$$i_{cj}(k) = i_{dc}(k) - \sum_{x=A,B,C} H_{xj} i_x(k) \tag{6}$$

where i_{dc} is the current of the DC bus. Variable H_{jx} depends on the switching variable and is defined as

$$H_{xj} = \begin{cases} 1 & if\ (S_x = 1 \,\&\, j = 1)\ or\ (S_x = -1 \,\&\, j = 2) \\ 0 & otherwise \end{cases} \tag{7}$$

where S_x represents the switching variable of phase x. It can be inferred that S_x has three possible values 1 (state P), 0 (state O), -1 (state N). Thus, there are 27 switching states in three-phase three-level inverters, including six long vectors, six medium vectors, six small vectors and one zero vector, as depicted in Fig. 2. It can be seen that both zero and small vectors have redundant switching states.

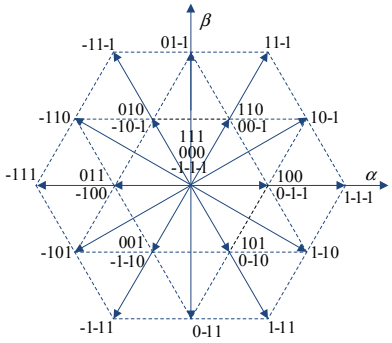

Fig. 2. Space vector diagram of a 3LT²I

B. Cost Function Minimization

In order to track the reference currents and balance the NPPs of the 3LT²I, the cost function in conventional FCS-MPC method for the 3LT²I is expressed as

$$\begin{aligned} g = &\left| i_\alpha^*(k) - i_\alpha(k+1) \right| + \left| i_\beta^*(k) - i_\beta(k+1) \right| \\ &+ \lambda_{dc} \left| V_{c1}(k+1) - V_{c2}(k+1) \right| \end{aligned} \tag{8}$$

where $i_\alpha^*(k)$ and $i_\beta^*(k)$ are the reference currents at the instant k. Weighting factor λ_{dc} handles the relation between terms dedicated to reference current tracking and NPPs balance. A larger value of λ_{dc} implies greater priority to the objective of NPPs balance. The future values of the grid currents and DC link capacitor voltages are predicted for all the 27 switching states and the one which minimizes the cost function is is selected and applied during the next control period.

C. Delay Compensation

However, the unavoidable calculation delay in digital implementation has significant influence on the performance of the 3LT²I. In order to compensate the calculation delay in digital control [23], the cost function considers the current errors and difference of the DC link capacitor voltages at instant $k+2$, which is expressed as

$$\begin{aligned} g = &\left| i_\alpha^*(k) - i_\alpha(k+2) \right| + \left| i_\beta^*(k) - i_\beta(k+2) \right| \\ &+ \lambda_{dc} \left| V_{c1}(k+2) - V_{c2}(k+2) \right| \end{aligned} \tag{9}$$

where the predicted currents i_α(k+2), i_β(k+2) and *the* predicted voltages V_{c1}(k+2), V_{c2}(k+2) are *obtained by* shifting the predicted values at instant $k+1$ one-step forward.

III. ANALYSIS OF CMV FOR 3LT²IS CONSIDERING DEAD TIME EFFECTS

The CMV of the 3LT²I, defined as the potential between the grid neutral n and the neutral point of the DC bus, can be expressed with the pole voltages with respect to the neutral point of the DC bus as [9]

$$u_{\text{cmv}} = \frac{u_{AO} + u_{BO} + u_{CO}}{3} \tag{10}$$

Since the 3LT^{2}I takes the leg voltages on the discrete voltage levels with $U_{dc}/2$ (state *P*), $-U_{dc}/2$ (state *N*) and an extra 0 (state *O*) compared with two-level inverters, the CMV generated by the 3LT^{2}I becomes $\pm U_{dc}/2$, $\pm U_{dc}/3$, $\pm U_{dc}/6$ and 0. Thus, the 27 switching states can be divided into 7 groups by different CMV values where the relationships between the switching states and CMV are summarized in Table I.

TABLE I. RELATIONSHIP BETWEEN SWITCHING STATES AND CMV

Switching States（$S_AS_BS_C$）	u_{CMV}	Group
111	$U_{DC}/2$	*G1*
110, 011, 101	$U_{DC}/3$	*G2*
100, 010, 001, 11-1, -111, 1-11	$U_{DC}/6$	*G3*
000, 10-1, 01-1, -110, -101, 0-11, 1-10	*0*	*G4*
00-1, -100, 0-10, 1-1-1, -11-1, -1-11	$-U_{DC}/6$	*G5*
0-1-1, -10-1, -1-10	$-U_{DC}/3$	*G6*
-1-1-1	$-U_{DC}/2$	*G7*

In the conventional FCS-MPC method, all the 27 switching states are utilized to perform the optimization in every control period which may result in large CMV fluctuations according to Table I. However, it can be observed that the 7 switching states from *G4* corresponding to 6 medium and 1 zero vectors (6MV1Z) generate zero CMV. Therefore, the CMV can be theoretically confined to zero if only VVs from 6MV1Z are adopted to perform the optimization in every control period. The switch state graph of the FCS-MPC based 6MV1Z method is shown in Fig. 3.

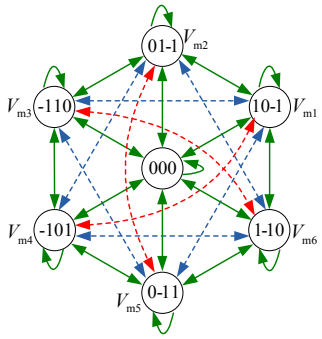

Fig. 3. Switch state graph of 6MV1Z

It can be seen that any VV is permitted to be applied in the next control period with the FCS-MPC method. Thus, the FCS-MPC method can lead to simultaneous commutations in two or three inverter legs which is unlike the well-known space vector PWM method where only one leg is involved at every switching transition. As the uncontrollable grid current flows through the freewheeling diode during the dead time, spontaneous CMV fluctuations may be generated. Since the output voltage of each phase depends on the polarities of the grid current during the dead time. One fundamental period of the grid currents are classified into six sections in which none of the grid currents change their polarities, as shown in Fig. 4.

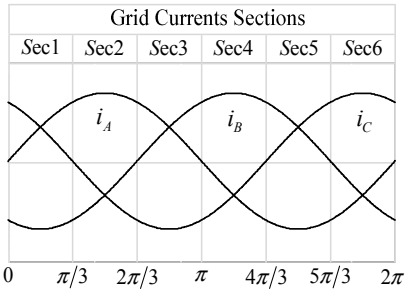

Fig. 4. Classification of one fundamental period of grid currents

As to the case where two legs of the 3LT^{2}I are involved in the switching transition, it can be summarized that the CMV of the 3LT^{2}I keeps zero during the dead time if the output currents of the operation legs are with different polarities. However, same polarity of the output currents for the operation legs results in $\pm U_{dc}/6$ or $\pm U_{dc}/3$ unplanned CMV fluctuations during the dead time. Fig. 5 show examples of the switching transition where two legs of the 3LT^{2}I are involved.

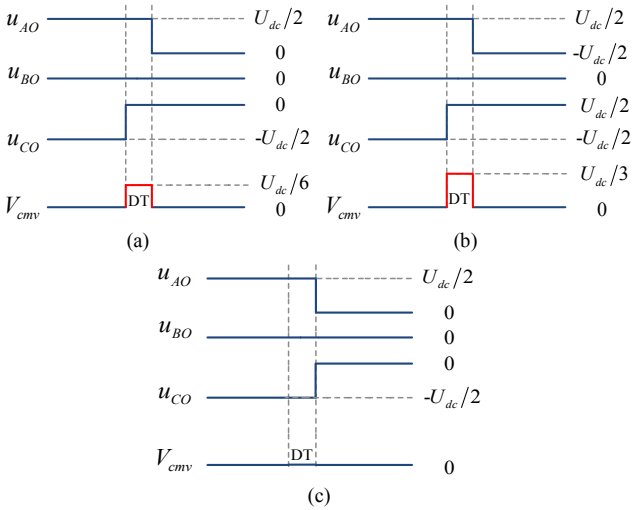

Fig. 5. Examples of switching transitions: (a) V_{m1} and V_0 in *Sec 4*, (b) V_{m1} and V_{m4} in *Sec 4*, (c) V_{m1} and V_0 in *Sec 2*.

Similarly, as to the case where three legs of the 3LT^{2}I are involved in the switching transition, it can be inferred that the CMV of the 3LT^{2}I keeps zero during the dead time if the output currents of the two operation legs which correspond to a state transition PO and a state transition ON are with the same polarities. Otherwise, $\pm U_{dc}/6$ unplanned CMV fluctuations are generated.

IV. PROPOSED FCS-MPC METHOD TO ELIMINATE CMV

The above analysis shows that CMV fluctuations may be generated during the dead time zone. In order to eliminate the potential CMV fluctuations during dead time, a new FCS-MPC based method is proposed based on the 6MV1Z method. The

candidate VVs for the proposed CMV elimination (CMV-EL) method are chosen by pre-excluding the VVs which will cause CMV fluctuation during the dead time zone from 6MV1Z. The candidate VVs various from different sections and are summarized in Table II.

TABLE II. CANDIDATE VVS FOR THE PROPOSED CMV-EL STRATEGY

Current VV	*Candidate VV Combinations*		
	Sec 1 & Sec 4	*Sec 2 & Sec 5*	*Sec 3 & Sec 6*
V_0	$V_0\ V_{m2}\ V_{m3}\ V_{m5}\ V_{m6}$	$V_0\ V_{m1}\ V_{m3}\ V_{m4}\ V_{m6}$	$V_0\ V_{m1}\ V_{m2}\ V_{m4}\ V_{m5}$
V_{m1}	$V_{m1}\ V_{m2}\ V_{m6}$	$V_0\ V_{m1}\ V_{m2}\ V_{m3}\ V_{m4}$	$V_0\ V_{m1}\ V_{m4}\ V_{m5}\ V_{m6}$
V_{m2}	$V_0\ V_{m1}\ V_{m2}\ V_{m5}\ V_{m6}$	$V_1\ V_{m2}\ V_{m3}$	$V_0\ V_{m2}\ V_{m3}\ V_{m4}\ V_{m5}$
V_{m3}	$V_0\ V_{m3}\ V_{m4}\ V_{m5}\ V_{m6}$	$V_0\ V_{m1}\ V_{m2}\ V_{m3}\ V_{m6}$	$V_{m2}\ V_{m3}\ V_{m4}$
V_{m4}	$V_{m3}\ V_{m4}\ V_{m5}$	$V_0\ V_{m1}\ V_{m4}\ V_{m5}\ V_{m6}$	$V_0\ V_{m1}\ V_{m2}\ V_{m3}\ V_{m4}$
V_{m5}	$V_0\ V_{m2}\ V_{m3}\ V_{m4}\ V_{m5}$	$V_{m4}\ V_{m5}\ V_{m6}$	$V_0\ V_{m1}\ V_{m2}\ V_{m5}\ V_{m6}$
V_{m6}	$V_0\ V_{m1}\ V_{m2}\ V_{m3}\ V_{m6}$	$V_0\ V_{m3}\ V_{m4}\ V_{m5}\ V_{m6}$	$V_1\ V_{m5}\ V_{m6}$

As shown in Table II, it can be seen that the candidate VVs are the same for *Sec 1* and *Sec 2*, *Sec 3*and *Sec 4*, *Sec 5*and *Sec 6*, respectively.

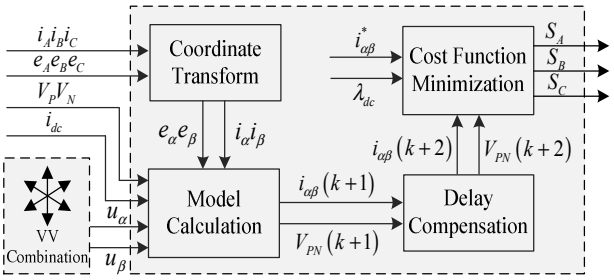

Fig. 6. Block diagram of the proposed CMV-EL method

Note that the current flow through the neutral point of the DC bus for all the candidate VV combinations shown in Table II always includes i_A, i_B and i_C. For a balanced three-phase system, the output current of each phase satisfy $i_A + i_B + i_C = 0$, which means that among i_A, i_B and i_C, two of them always have the opposite polarity with the third one. Since that different polarities of the current flow through the neutral point has different effects to the potential of the neutral point. Therefore, it is readily to see that the proposed CMV-EL method has the ability to control the potential of the neutral point. Fig. 6 shows the whole control block diagram of the proposed CMV-EL method.

V. EXPERIMENTAL RESULTS

In order to validate the effectiveness of the proposed FCS-MPC based CMV-EL method, experiments are carried out on a prototype built in laboratory and the entire algorithms of the proposed CMV-EL method are implemented on a DSP chip TMS320F28335. The system and control parameters used in the experimental study are fully listed in Table III.

TABLE III. SYSTEM AND CONTROL PARAMETERS IN EXPERIMENT

Symbol	Quantity	Value
L	Filter inductance	10mH
R	Line resistance	1.7Ω
e_{peak}	Grid voltage	20V
U_{DC}	DC-link voltage	100V
C	DC-link Capacitance	2mF
f	fundamental frequency	50Hz
T_s	Control period	100μs
t_d	Dead time	3μs

Fig. 7(a) presents the experimental waveform of the CMV obtained by the proposed CMV-EL method. Here, it should be noted that the CMV curve is calculated by $(V_{AN}+V_{BN}+V_{CN})/3-V_{DC}/2$, where V_{xN} (x=A, B, C) is measured by oscilloscope. It is seen that less CMV fluctuations are generated due to the polarity misjudgement of the grid currents during zero crossing in the experimental study. Fig.7(b) shows the output voltage of the 3LT^{2}I obtained by the proposed CMV-EL method. Both load current tracking and NPP balance control can achieve satisfactory performances as shown in Fig. 7(c) and Fig. 7(d), respectively.

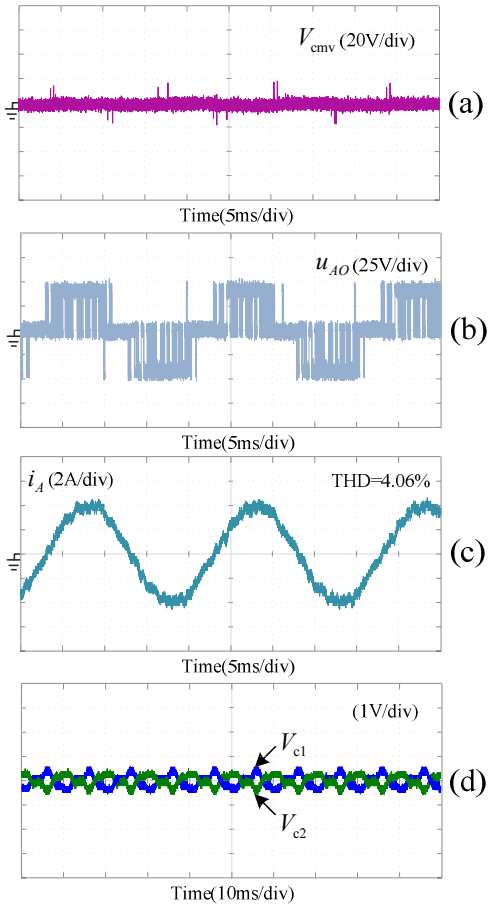

Fig. 7. Experimental waveforms of the proposed CMV-EL method: (a) the leakage current (i_L), (b) common-mode voltage, (c) grid currents i_A and (d) fluctuations of the NPP.

Fig. 8 shows the experimental result of the dynamic responses obtained by the proposed CMV-EL method. It is observed that the grid currents generated by the proposed CMV-EL method can follow the changes of the reference with fast dynamics for step changes in both magnitude and frequency.

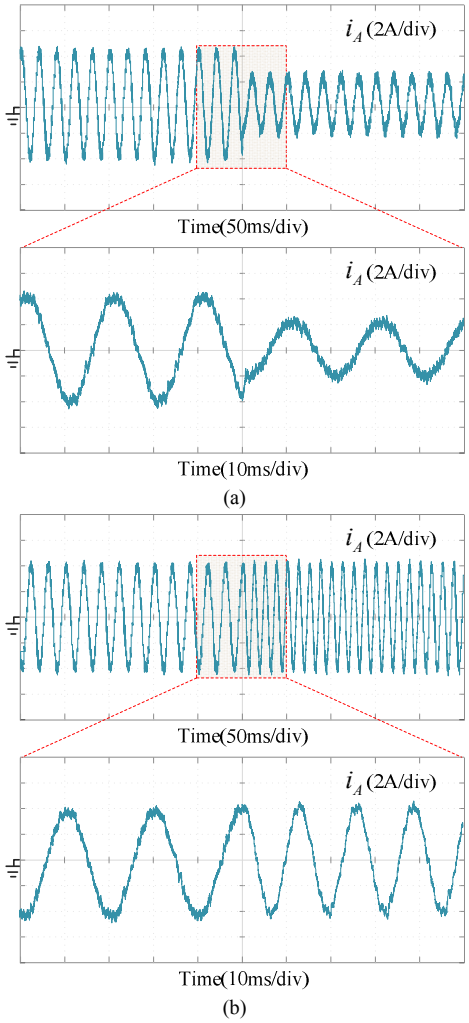

Fig. 8. Experimental waveforms of the phase current with step changes: (a) with a magnitude step change from 4A to 2A, (b) with a frequency step change from 50Hz to 80Hz.

VI. CONCLUSION

This paper proposed a new FCS-MPC based common-mode voltage elimination (CMV-EL) method for 3LT^{2}I with considering dead time effects. The dead time effects on the FCS-MPC method are analyzed and the candidate VVs for the proposed FCS-MPC based CMV-EL method are redesigned by pre-excluding the VVs which will cause CMV fluctuations during the dead time zone. Experimental results are presented to verify that the proposed CMV-EL method can effectively eliminate the CMV as well as control the grid current and balance the NPPs.

REFERENCES

[1] D.Meneses, F.Blaabjerg, O.GarciA and J.A.Cobos, "Review and comparison of step-up transformerless topologies for photovoltaic ac-module application," *IEEE Trans. Power Electron*., vol.28, no.6, pp.2649 -2663, Jun.2013.

[2] K.Li, H.Xu, Q.Ma and J.Zhao, "Hierarchy control of power quality for wind–battery energy storage system," *IET Power Electron*., vol.7, no.8, pp.2123-2132, Aug.2014.

[3] R. Teichmann, S. Bernet, "A comparison of three-level converters versus two-level converters for low-voltage drives traction and utility applications", *IEEE Trans. Ind. Appl*., vol. 41, no. 3, pp. 855-865, May/Jun. 2005.

[4] Y. Atia and M. Salem, "Microcontroller-based improved predictive current controlled VSI for single-phase grid-connected systems," *J. Power Electron*., vol. 13, no. 6, pp. 1016–1023, Nov. 2013.

[5] M. P. Kazmierkowski, R. Krishnan, and F. Blaabjerg,Control in Power Electronics. New York, NY, USA: Academic, 2002.

[6] G. Park, S. Lee, S. Jin, and S. Kwak, "Integrated modeling and analysis of dynamics for electric vehicle powertrains," *Expert Syst. Appl*., vol. 41, no. 5, pp. 2595–2607, Apr. 2014.

[7] J. M. Erdman, R. J. Kerkman, D. W. Schlegel, and G. L. Skibinski, "Effect of PWM inverters on AC motor bearing currents and shaft voltages," *IEEE Trans. Ind. Appl*., vol. 32, no. 2, pp. 250–259, Feb. 1996.

[8] J. D. Barros, J. F. A. Silva and É. G. A. Jesus, "Fast-predictive optimal control of NPC multilevel converters," *IEEE Trans. Ind. Electron*., vol. 60, no. 2, pp. 619–627, Feb. 2013.

[9] S. Kwak and J. C. Park, "Predictive control method with future zero-sequence voltage to reduce switching losses in Three-Phase voltage source inverters," *IEEE Trans. Power Electron*., vol. 30, no. 3, Mar. 2015.

[10] J. Rodríguez, J. Pontt, C. A. Silva, P. Correa, P. Lezana, P. Cortés and U. Ammann, "Switching strategy based on model predictive control of VSI to obtain high efficiency and balanced loss distribution," *IEEE Trans. Power Electron*., vol. 29, no. 9, Sep. 2014.

[11] J. M. Erdman, R. J. Kerkman, D. W. Schlegel, and G. L. Skibinski, "Effect of PWM inverters on AC motor bearing currents and shaft voltages," *IEEE Trans. Ind. Appl*., vol. 32, no. 2, pp. 250–259, Mar./Apr. 1996.

[12] M. C. Cavalcanti, A. M. Farias, K. C. Oliveira, F. A. S. Neves and J. L. Afonso, "Eliminating Leakage Currents in Neutral Point Clamped Inverters for Photovoltaic Systems," in *IEEE Transactions on Industrial Electronics*, vol. 59, no. 1, pp. 435-443, Jan. 2012.

[13] R. M. Tallam, R. J. Kerkman, D. Leggate, and R. A. Lukaszewski, "Common-mode voltage reduction PWM methodfor AC Drives," *IEEE Trans. Ind. Appl*., vol. 46, no. 5, pp. 1959–1969, Sep./Oct. 2010.

[14] J. W. Kimball and M. Zawodniok, "Reducing common-mode voltage in three-phase sine-triangle PWM with interleaved carriers," *IEEE Trans. Power Electron*., vol. 26, no. 8, pp. 2229–2236, Aug. 2011.

[15] M. C. Cavalcantiet al., "Modulation techniques to eliminate leakage currents in transformerless three-phase photovoltaic systems,"*IEEE Trans. Ind. Electron*., vol. 57, no. 4, pp. 1360–1368, Apr. 2010.

[16] X. Wu, G. Tan, Z. Ye, Y. Liu and S. Xu, "Optimized Common-Mode Voltage Reduction PWM for Three-Phase Voltage Source Inverters, " in *IEEE Transactions on Power Electronics*, vol. 31, no. 4, pp. 2959-2969, April 2016.

[17] V. Yaramasu, M. Rivera, M. Narimani, B. Wu, and J. Rodriguez, "Model predictive approach for a simple and effective load voltage control of four-leg inverter with an output *lc* filter," *IEEE Trans. Ind. Electron*., vol. 61,no. 10, pp. 5259–5270, Oct. 2014.

[18] R. Ramirez, J. Espinoza, F. Villarroel, E. Maurelia, and M. Reyes, "A novel hybrid finite control set model predictive control scheme with reduced switching," *IEEE Trans. Ind. Electron*., vol. 61, no. 11, pp. 5912–5920, Nov. 2014.

[19] S. Kwak and S. Mun, "Model predictive control methods to reduce common-mode voltage for three-phase voltage source inverters," *IEEE Trans. Power Electron*., vol. 30, no. 9, pp. 5019–5035, Sep. 2015.

[20] S. Kwak and J. Park, "Model predictive direct power control with vector preselection technique for highly efficient active rectifiers," *IEEE Trans. Ind. Informat*, vol. 11, no. 1, pp. 44–52, Feb. 2015.

[21] L. Guo, X. Zhang, S. Yang, Z. Xie and R. Cao, "A Model Predictive Control-Based Common-Mode Voltage Suppression Strategy for Voltage-Source Inverter, " in *IEEE Transactions on Industrial Electronics*, vol. 63, no. 10, pp. 6115-6125, Oct. 2016.

[22] X. Xing, A. Chen, Z. Zhang, J. Chen and C. Zhang, "Model predictive control method to reduce common-mode voltage and balance the neutral-point voltage in three-level T-type inverter, " *2016 IEEE Applied Power Electronics Conference and Exposition (APEC)*, Long Beach, CA, 2016, pp. 3453-3458.

[23] P. Cortes, J. Rodriguez, C. Silva and A. Flores, "Delay Compensation in Model Predictive Current Control of a Three-Phase Inverter, " in *IEEE Transactions on Industrial Electronics*, vol. 59, no. 2, pp. 1323-1325, Feb. 2012.